Impact of dimension-eight SMEFT contributions: A case study

Sally Dawson,[1] Samuel Homiller,[2] and Matthew Sullivan[1]
[1]*Department of Physics, Brookhaven National Laboratory, Upton, New York 11973, USA*
[2]*Physics Department, Harvard University, Cambridge, Massachusetts 02138, USA*

(Received 19 October 2021; accepted 11 November 2021; published 13 December 2021)

The use of the Standard Model effective field theory Lagrangian to quantify possible Beyond the Standard Model (BSM) effects is standard in LHC and future collider studies. One of the usual assumptions is to truncate the expansion with the dimension-six operators. The numerical impact of the next terms in the series, the dimension-eight operators, is unknown in general. We consider a specific BSM model containing a charge-2/3 heavy vectorlike quark and compute the operators generated at dimension eight. The numerical effects of these operators are studied for the $t\bar{t}h$ process, where they contribute at tree level and we find effects at the $\mathcal{O}(0.5\text{–}2\%)$ level for allowed values of the parameters.

DOI: 10.1103/PhysRevD.104.115013

I. INTRODUCTION

One of the goals of the high luminosity LHC (HL-LHC) running is a precision physics program that enables a detailed comparison of theoretical and experimental predictions. Lacking the experimental discovery of any new particles, the tool of choice is the Standard Model effective field theory (SMEFT) which assumes that the gauge symmetries and particles of the Standard Model provide an approximate description of weak scale physics [1]. Deviations from the Standard Model (SM) predictions are parametrized in terms of an infinite tower of higher dimension operators,

$$\mathcal{L} \sim \mathcal{L}_{\rm SM} + \sum_n \sum_i \frac{C_i^{(n)}}{\Lambda^{n-4}} O_i^{(n)}, \tag{1}$$

where Λ is a high energy scale where some unknown ultraviolet (UV) complete model is presumed to exist. All of the new physics information resides in the coefficient functions, $C_i^{(n)}$, which can be extracted from experimental data.

The SMEFT amplitude for a tree-level scattering process can be written schematically as,

$$\mathcal{A} \sim \mathcal{A}_{\rm SM} + \sum_i \frac{C_i^{(6)}}{\Lambda^2} \mathcal{A}_i^{(6)} + \sum_i \frac{C_i^{(8)}}{\Lambda^4} \mathcal{A}_i^{(8)} + \cdots, \tag{2}$$

where $\mathcal{A}_{\rm SM}$, $\mathcal{A}_i^{(6)}$, and $\mathcal{A}_i^{(8)}$ are the SM, dimension-six, and dimension-eight contributions, respectively.[1] Squaring the amplitude, a physical cross section takes the form of an integral over the appropriate phase space, dPS,

$$\begin{aligned} d\sigma \sim \int (\mathrm{dPS}) \Bigg\{ & |\mathcal{A}_{\rm SM}|^2 + \frac{2}{\Lambda^2} \mathrm{Re}\left(\sum C_i^{(6)} \mathcal{A}_i^{(6)} \mathcal{A}_{\rm SM}^* \right) \\ & + \frac{1}{\Lambda^4} \mathrm{Re}\left(\sum_{i,j} C_i^{(6)} C_j^{(6)*} \mathcal{A}_i^{(6)} \mathcal{A}_j^{(6)*} \right) \\ & + \frac{2}{\Lambda^4} \mathrm{Re}\left(\sum_i C_i^{(8)} \mathcal{A}_i^{(8)} \mathcal{A}_{\rm SM}^* \right) \Bigg\} + \ldots \end{aligned} \tag{3}$$

It is immediately apparent that the squares of the dimension-six contributions are formally of the same power counting in $1/\Lambda^4$ as the interference of the dimension-eight terms with the SM result unless assumptions are made about the relative sizes of the contributions. If the process being studied is extremely well constrained (as is the case for the electroweak precision observables), it may be sufficient to include only the $1/\Lambda^2$ contributions, as the $1/\Lambda^4$ terms are negligible in this case [2–4]. Alternatively, the SMEFT could result from a strongly interacting theory at the UV scale where the $\mathcal{A}_{\rm SM}\mathcal{A}^{(8)}/\Lambda^4$ terms are suppressed relative to the $|\mathcal{A}^{(6)}|^2/\Lambda^4$ contributions [5,6]. There are, however, scenarios where the inclusion of the dimension-eight terms may be critical in order to obtain reliable results due to cancellations of the $|\mathcal{A}^{(6)}|^2/\Lambda^4$ terms in specific kinematic regimes [7]. There are also scenarios where new

[1]We neglect baryon and lepton number violating operators.

physics effects first arise at dimension eight, such as the $ZZ\gamma$ coupling [8,9]. Furthermore, in weakly coupled theories, there is generically no reason to expect the dimension-eight contributions to be suppressed.

In practice, the SMEFT series is usually terminated at dimension six and the amplitude is computed to $\mathcal{O}(1/\Lambda^2)$, generating $\mathcal{O}(1/\Lambda^4)$ contributions in cross sections. This leaves an uncertainty about the numerical relevance of the higher dimension operators. A complete basis for the dimension-eight operators now exists [10–14], making possible phenomenological studies of the effects of these operators. The literature, however, contains very few concrete examples of the effects of dimension-eight contributions. Studies of a subset of dimension-eight contributions to the Higgs boson plus jet production show a modest distortion of kinematic shapes at high p_T [15–19]. Reference [10] considers the dimension-eight contributions to Wh production and notes that quite large cancellations between the contributions of different dimension-eight operators are possible. In a similar vein, the authors of Ref. [20] compute Z pole observables to $\mathcal{O}(1/\Lambda^4)$ and find numerically significant effects. These examples consider the SMEFT coefficients as arbitrary unknown parameters. In a given UV model, however, the coefficients are predicted, and the conclusions that can be drawn from studies of SMEFT parameters depend sensitively on the relationships between the different coefficients at the UV scale [4,21,22].

In this paper, we discuss an example of UV physics where the coefficients of the dimension-six and dimension-eight operators can be computed in terms of a small number of input parameters, allowing us to assess the relevance of terms of $\mathcal{O}(1/\Lambda^4)$ arising from the dimension-eight operators. The example we consider contains a charge-2/3 vectorlike top quark (TVLQ) that is assumed to exist at the UV scale. Such particles occur in little Higgs models [23–25] and in many composite Higgs models [26–29], and represent a highly motivated scenario. Within the context of this model, the coefficients of the dimension-six and dimension-eight operators can be calculated using the covariant derivative expansion [30,31] and matched to the SMEFT. This allows for a detailed numerical analysis of the various approximations frequently used when computing observables in the SMEFT. We consider $t\bar{t}h$ associated production in the SMEFT limit of the TVLQ and are able to concretely determine the numerical relevance of the dimension-eight contributions to this process at tree level. The SM rate for tth production at the LHC is well known at next-to-leading order (NLO) QCD [32–35].

In Sec. II, we review the construction of the TVLQ model and we pay particular attention to the decoupling properties of the TVLQ model. The tree-level matching to the SMEFT at dimension eight is given in Sec. III. Phenomenological results for $t\bar{t}h$ at dimension eight in the SMEFT limit of the TVLQ are presented in Sec. IV, where we emphasize the importance of including the top decay products for SMEFT studies. We conclude with a discussion of the impact of our results in Sec. V. The appendixes include a short summary of the relevant dimension-eight interactions and a brief discussion of one-loop matching in the TVLQ model.

II. THE TVLQ MODEL

We consider an extension of the Standard Model with one additional vectorlike, charge-2/3 quark, denoted $\mathcal{T}_L^2$, $\mathcal{T}_R^2$, that can mix with the Standard-Model-like top quark, $\mathcal{T}_L^1, \mathcal{T}_R^1$, and we call this the TVLQ model. This model has been extensively studied in the literature [36–48] and we briefly summarize the salient points. The SM-like third-generation chiral fermions are

$$\psi_L = \begin{pmatrix} \mathcal{T}_L^1 \\ b_L \end{pmatrix}, \qquad \mathcal{T}_R^1, \qquad b_R, \tag{4}$$

with the usual Higgs Yukawa couplings,

$$\mathcal{L}_{\rm Yuk}^{\rm SM} = -\lambda_b \bar{\psi}_L H b_R - \lambda_t \bar{\psi}_L \tilde{H} \mathcal{T}_R^1 + \text{H.c.}, \tag{5}$$

where $\tilde{H}_i = \epsilon_{ij} H_j^*$. Note that we will distinguish between the SM-like Yukawa couplings λ_b, λ_t in Eq. (5), their SM values $Y_b = \sqrt{2} m_b/v$, $Y_t = \sqrt{2} m_t/v$, with m_b and m_t being the physical quark masses, and the Yukawa couplings derived in the SMEFT construction of Sec. III. As usual, $v = (\sqrt{2} G_F)^{-1/2}$.

The most general fermion mass terms for the charge-2/3 quarks are

$$\mathcal{L} = \mathcal{L}_{\rm Yuk}^{\rm SM} - \lambda_T \bar{\psi}_L H^c \mathcal{T}_R^2 - m_{12} \bar{\mathcal{T}}_L^2 \mathcal{T}_R^1 - m_{\mathcal{T}} \bar{\mathcal{T}}_L^2 \mathcal{T}_R^2 + \text{H.c.} \tag{6}$$

Since $\mathcal{T}_R^2$, $\mathcal{T}_R^1$ have identical quantum numbers, the m_{12} term can be set to zero by a redefinition of the fields. The charge-2/3 sector is thus described by three parameters: λ_t, λ_T, and $m_{\mathcal{T}}$.

The physical fields, t and T, with masses m_t and M_T, are found by diagonalizing the mass matrix with two unitary matrices,

$$\begin{pmatrix} t \\ T \end{pmatrix}_{L,R} = \begin{pmatrix} \cos\theta_{L,R} & -\sin\theta_{L,R} \\ \sin\theta_{L,R} & \cos\theta_{L,R} \end{pmatrix} \begin{pmatrix} \mathcal{T}_L^1 \\ \mathcal{T}_L^2 \end{pmatrix}_{L,R}, \tag{7}$$

and we use the shorthand $c_{L,R} \equiv \cos\theta_{L,R}$ and $s_{L,R} \equiv \sin\theta_{L,R}$.

Useful relationships between the Lagrangian and physical parameters are

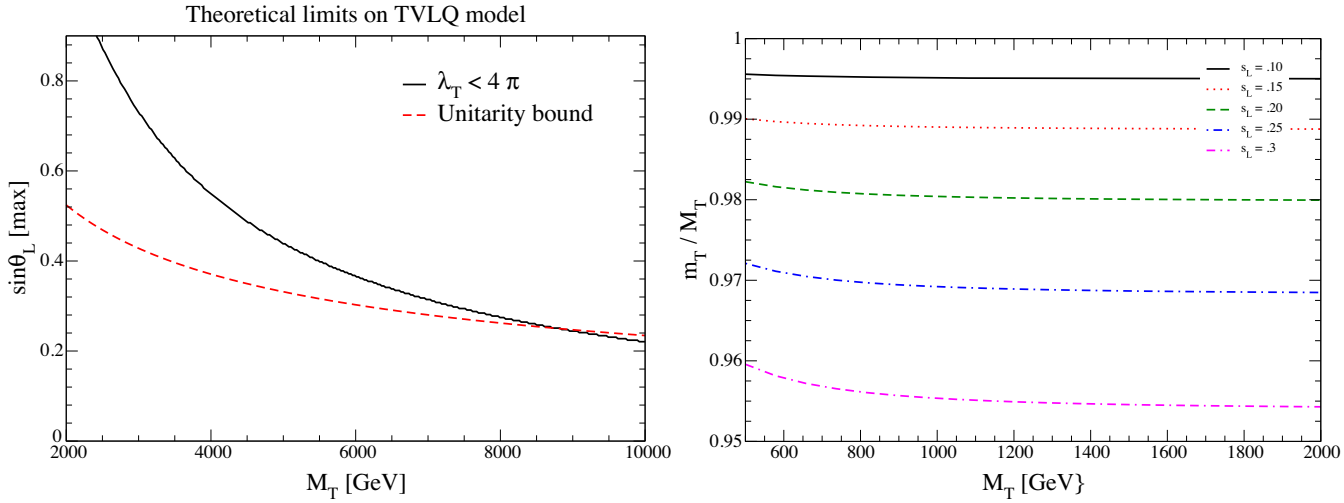

FIG. 1. Left: upper limit on s_L as a function of M_T from perturbativity and unitarity. Right: relationship between the Lagrangian mass, m_T, and the physical mass, M_T, for fixed $\sin\theta_L \equiv s_L$.

$$\begin{aligned}
\frac{\lambda_t v}{\sqrt{2}} &= c_L c_R m_t + s_L s_R M_T = \frac{s_R}{s_L} M_T \\
\frac{\lambda_T v}{\sqrt{2}} &= -s_R c_L m_t + s_L c_R M_T = \frac{s_R c_L}{m_t}(M_T^2 - m_t^2) \\
m_T &= s_L s_R m_t + c_L c_R M_T = \frac{s_R}{s_L m_t}(s_L^2 m_t^2 + c_L^2 M_T^2) \\
\tan\theta_R &= \frac{m_t}{M_T}\tan\theta_L. \qquad (8)
\end{aligned}$$

The following relationships follow from Eq. (8):

$$\begin{aligned}
\frac{\lambda_T v}{\sqrt{2} m_T} &= \frac{c_L s_L (1-x)}{\sqrt{1 - s_L^2(1-x)}} \\
\frac{\lambda_t v}{\sqrt{2}} &= \frac{m_t}{\sqrt{1 - s_L^2(1-x)}} \\
\frac{\lambda_T v}{\sqrt{2}} &= M_T \frac{s_L c_L (1-x)}{\sqrt{(1 - s_L^2(1-x))}} \\
m_T &= M_T \sqrt{1 - s_L^2(1-x)}, \qquad (9)
\end{aligned}$$

with $x \equiv m_t^2/M_T^2$. From Eq. (9), it is clear that for fixed s_L, λ_T will become nonperturbative at large M_T. In Fig. 1 (lhs), we show the upper limit on s_L from the requirement that $\lambda_T \lesssim 4\pi$, along with the unitarity limit from $\bar{T}T \to \bar{T}T$ of $s_L^2 \lesssim 550\ \text{GeV}/M_T$ [49]. The $M_T \to \infty$ limit therefore requires $s_L \to 0$ for a weakly interacting theory. We also observe that the expansions in $1/M_T^2$ and $1/m_T^2$ have different counting in inverse mass dimensions for fixed s_L,

$$\frac{1}{m_T^2} = \frac{1}{M_T^2} + \frac{s_L^2}{M_T^2}\left(1 - \frac{m_t^2}{M_T^2}\right), \qquad (10)$$

as is demonstrated in Fig. 1 (rhs). The ratio m_T/M_T quickly goes to its asymptotic limit as $M_T \to \infty$, and for $s_L \sim 0.2$, the ratio approaches ~ 0.98.

The relations of Eq. (9) can be inverted [36] as

$$\begin{aligned}
m_t^2 &= \frac{(\lambda_t^2 + \lambda_T^2)v^2}{4} \\
&\quad + \frac{m_T^2}{2}\left[1 - \sqrt{\left(1 + \frac{(\lambda_t^2 + \lambda_T^2)v^2}{2m_T^2}\right)^2 - \frac{2\lambda_t^2 v^2}{m_T^2}}\right] \\
M_T^2 &= \frac{m_T^2}{m_t^2}\left(\frac{\lambda_t^2 v^2}{4}\right) \\
s_L &= \frac{\lambda_T v}{\sqrt{2} m_T} \frac{1}{\sqrt{(1 - \frac{m_t^2}{m_T^2})^2 + \frac{\lambda_T^2 v^2}{2m_T^2}}}. \qquad (11)
\end{aligned}$$

In our phenomenological studies we will switch between Lagrangian parameters and the physical parameters to illustrate various points. We remind the reader that the physical masses are m_t and M_T with $m_t \ll M_T$, and that m_T is the Lagrangian parameter.

The oblique parameters place stringent limits on the parameters of the TVLQ. In Fig. 2, we update the results of Ref. [37], include the global fit results of Ref. [21], and compare these with the direct search limits from $T\bar{T}$ pair production [50,51] (which are independent of s_L). We also show a comparison of current searches with projections for the HL-LHC and FCC-hh and note that the HL-LHC will be sensitive to $M_T \sim 1.7$ TeV, while the hadronic version of the future circular collider (FCC-hh) can probe up to ~6 TeV [52,53].[2]

[2]We note that $g^* = 2s_L$.

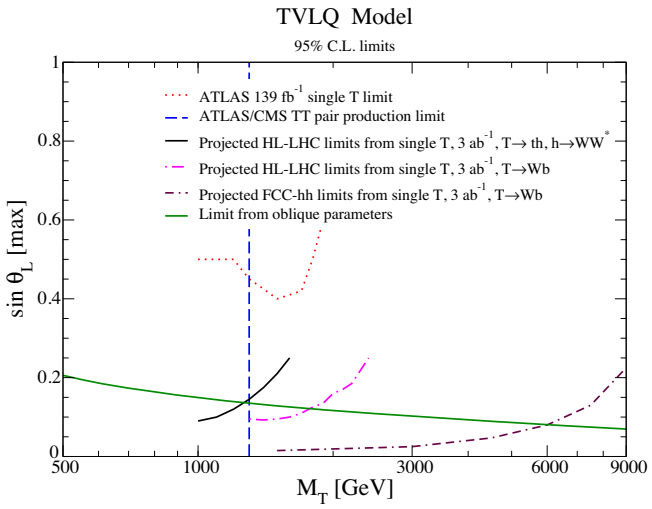

FIG. 2. LHC 95% exclusion limits on TVLQ masses from single T production with $T \to ht, Zt$ as a function of s_L [54] (red dotted line), limits from $T\bar{T}$ production with $T \to th, Zt, Wb$ [50,51] (blue dashed), projected limits from single T production at HL-LHC with $T \to th, h \to WW^*$ [52] (black solid), projected limits at HL-LHC from single T production with $T \to Wb$ [53] (magenta dot-dashed), and projected limits at FCC-hh ($\sqrt{S} = 100$ TeV) from single T production with $T \to Wb$ [53] (purple long dot-dashed). The region above the curves is excluded.

III. MATCHING TO SMEFT AT DIMENSION-EIGHT

In this section, we consider the $M_T \to \infty$ limit of the TVLQ model and perform the tree-level matching to the SMEFT, extending the dimension-six results [46,47,55] to dimension eight. Since the full UV model depends on only three unknown parameters, it is particularly simple. We use the covariant derivative expansion [30,31] to integrate the heavy T out of the theory and generate the effective operators at dimension six and dimension eight. The resulting Lagrangian involving the SM-like top quark t is

$$\mathcal{L}_t \equiv \mathcal{L}_{\rm kin} + \mathcal{L}_Y + \mathcal{L}_6 + \mathcal{L}_8, \tag{12}$$

where

$$\begin{aligned}
\mathcal{L}_{\rm kin} &= i\bar{\psi}_L \not{D}\psi_L + i\bar{t}_R \not{D} t_R \\
&= \frac{i}{2}[\bar{\psi}_L(\not{D}\psi_L) - (\bar{\psi}_L \overleftarrow{\not{D}})\psi_L] + i\bar{t}_R \not{D} t_R \\
\mathcal{L}_Y &= -\lambda_t \bar{\psi}_L \tilde{H} t_R + \text{H.c.} \\
\mathcal{L}_6 &= \frac{i}{2}\frac{\lambda_T^2}{m_T^2}\bar{\psi}_L \tilde{H} \not{D}(\tilde{H}^\dagger \psi_L) + \text{H.c.} \\
\mathcal{L}_8 &= -\frac{i}{2}\frac{\lambda_T^2}{m_T^4}\bar{\psi}_L \tilde{H} \not{D}^3(\tilde{H}^\dagger \psi_L) + \text{H.c.},
\end{aligned} \tag{13}$$

and where $\not{D} \equiv \gamma^\mu D_\mu$. The covariant derivative D_μ is defined as $\partial_\mu - i\frac{g}{2}YB_\mu - ig_W\tau_a W_\mu^a - ig_s T_a G_\mu^a$, with hypercharge Y, $SU(2)$ generators τ_a, and $SU(3)$ generators T_a. The dimension-six term, L_6, generates a nonstandard normalization for the top quark kinetic energy term after electroweak symmetry breaking and the expansion of the Higgs field around its vev, so we make the gauge invariant field redefinition [56,57]

$$\psi_{L,i} \to \left(\psi_{L,i} - \frac{\lambda_T^2}{2m_T^2}(\tilde{H}_i \tilde{H}_j^\dagger)\psi_{L,j}\right), \tag{14}$$

where i, j are $SU(2)$ indices. This brings the top quark kinetic energy into the canonical form.

After making the field redefinition of Eq. (14),

$$\begin{aligned}
i\bar{\psi}_L \not{D}\psi_L + \mathcal{L}_6 &\to i\bar{\psi}_L \not{D}\psi_L + \frac{i\lambda_T^2}{2m_T^2}[(\bar{\psi}_L\tilde{H})(\not{D}\tilde{H}^\dagger)\psi_L - \bar{\psi}_L(\not{D}\tilde{H})\tilde{H}^\dagger\psi_L] + \delta\mathcal{L}_{8a} \\
&= i\bar{\psi}_L \not{D}\psi_L + \frac{i\lambda_T^2}{4m_T^2}[(\bar{\psi}_L\gamma^\mu\psi_L)(H^\dagger D_\mu H - (D_\mu H^\dagger)H) \\
&\quad - (\bar{\psi}_L\gamma^\mu\tau^a\psi_L)(H^\dagger\tau^a D_\mu H - (D_\mu H^\dagger)\tau^a H)] + \delta\mathcal{L}_{8a} \\
&= i\bar{\psi}_L \not{D}\psi_L + \frac{i\lambda_T^2}{4m_T^2}[O_{Ht}^{1,(6)} - O_{Ht}^{3,(6)}] + \delta\mathcal{L}_{8a} \\
\delta\mathcal{L}_{8a} &\equiv \frac{i\lambda_T^4}{8m_T^4}[3\not{D}(\bar{\psi}_L\tilde{H})\tilde{H}^\dagger\tilde{H}\tilde{H}^\dagger\psi_L + \bar{\psi}_L\tilde{H}\tilde{H}^\dagger(\not{D}\tilde{H})\tilde{H}^\dagger\psi_L + \text{H.c.}] \\
&= \frac{\lambda_T^4}{8m_T^4}[-3\lambda_t O_{quH^5}^{(8)} + 3(H^\dagger H)\bar{\psi}_L(i\not{D}\tilde{H})\tilde{H}^\dagger\psi_L + \bar{\psi}_L\tilde{H}\tilde{H}^\dagger(i\not{D}\tilde{H})\tilde{H}^\dagger\psi_L + \text{H.c.}] \\
\mathcal{L}_Y &\to -\lambda_t\bar{\psi}_L\tilde{H}t_R\left[1 - \frac{\lambda_T^2}{2m_T^2}(H^\dagger H)\right] + \text{H.c.} \\
&\equiv \left[-\lambda_t\bar{\psi}_L\tilde{H}t_R + \frac{\lambda_t\lambda_T^2}{2m_T^2}O_{tH}^{(6)} + \text{H.c.}\right],
\end{aligned} \tag{15}$$

TABLE I. Operators appearing in Eq. (15) where ψ_L is the (t,b) doublet, $H^\dagger \overleftrightarrow{D}_\mu H \equiv H^\dagger D_\mu H - (D_\mu H^\dagger)H$, and $H^\dagger \overleftrightarrow{D}^a_\mu H \equiv H^\dagger D_\mu \sigma^a H - (D_\mu H^\dagger \sigma^a)H$.

Dimension-six	
$O_{Ht}^{1,(6)}$	$(H^\dagger i\overleftrightarrow{D}_\mu H)(\bar{\psi}_L \gamma^\mu \psi_L)$
$O_{Ht}^{3,(6)}$	$(H^\dagger i\overleftrightarrow{D}^a_\mu H)(\bar{\psi}_L \tau^a \gamma^\mu \psi_L)$
$O_{tH}^{(6)}$	$(H^\dagger H)\bar{\psi}_L \tilde{H} t_R$
Dimension-eight	
$O_{quH^5}^{(8)}$	$(H^\dagger H)^2 \bar{\psi}_L \tilde{H} t_R$

where in the second line of Eq. (15), $SU(2)$ identities are used to put the dimension-six contributions in a standard form. Note that Eq. (15) contains dimension-eight interactions in addition to those of the dimension-eight operator of $\mathcal{L}_8$. Repeated use of the SM equations of motion on the dimension-eight term, $\delta\mathcal{L}_{8a}$, yields the second line of the expression for δL_{8a} in Eq. (15). We have not simplified the dimension-eight contributions with derivatives on the Higgs doublet, since it is straightforward to use FeynRules [58,59] to determine the needed interactions for a given application. The operators are defined in Table I using the bases of Refs. [11,60].

We simplify the dimension-eight operator of Eq. (13) to extract the term contributing to the top quark Yukawa interaction,

$$\begin{aligned}\mathcal{L}_8 &\to \frac{\lambda_t^3 \lambda_T^2}{2m_T^4}(H^\dagger H)^2(\bar{\psi}_L \tilde{H} t_R + \text{H.c.}) \\ &\quad + \text{terms with derivatives on } \tilde{H} \text{ or } \tilde{H}^\dagger \\ &\equiv \left(\frac{\lambda_t^3 \lambda_T^2}{2m_T^4}(H^\dagger H)^2 O_{quH^5}^{(8)} + \text{H.c.}\right) + \delta\mathcal{L}_{8b}, \end{aligned} \tag{16}$$

where the complete expression for $\delta\mathcal{L}_{8b}$ can be found in the Supplemental Material [61]. The contribution to $\delta\mathcal{L}_{8b}$ that is proportional to the strong coupling g_s is given in Appendix A, and the momentum dependence of the dimension-eight operators is clearly seen.

The complete SMEFT Lagrangian generated from the TVLQ model to dimension eight involving the top quark written in terms of the Lagrangian parameters is

$$\begin{aligned}\mathcal{L} &\equiv \mathcal{L}_4' + \mathcal{L}_6' + \mathcal{L}_8' \\ \mathcal{L}_4' &= \bar{\psi}_L(i\not{D})\psi_L + \bar{t}_R(i\not{D})t_R - (\lambda_t \bar{\psi}_L \tilde{H} t_R + \text{H.c.}) \\ \mathcal{L}_6' &= \left(\frac{\lambda_t \lambda_T^2}{2m_T^2} O_{tH}^{(6)} + \text{H.c.}\right) + \frac{\lambda_T^2}{4m_T^2}(O_{Ht}^{1,(6)} - O_{Ht}^{3,(6)}) \\ \mathcal{L}_8' &= \frac{\lambda_t \lambda_T^2}{8m_T^4}(4\lambda_t^2 - 3\lambda_T^2) O_{quH^5}^{(8)} + \delta\mathcal{L}_{8b} + \text{H.c.} \end{aligned} \tag{17}$$

We note that changing the input parameters from $(\lambda_t, \lambda_T, m_T)$ to (m_t, M_T, s_L) using Eq. (8) rearranges the counting in terms of inverse powers of the heavy mass [62]. Reference [62] argues that replacing the Lagrangian mass, m_T, with the physical mass, M_T, improves the agreement between the SMEFT predications and those of the corresponding UV complete model in many cases. A similar effect is found in the effective field theory (EFT) limit of the Higgs doublet model (2HDM) [63,64].

The terms contributing to the SMEFT relationship between the top mass and the Higgs boson top Yukawa coupling are

$$\mathcal{L} \sim -\lambda_t \bar{\psi}_L \tilde{H} t_R + \frac{C_{tH}^{(6)}}{m_T^2} O_{tH}^{(6)} + \frac{C_{quH^5}^{(8)}}{m_T^4} O_{quH^5}^{(8)} + \text{H.c.}, \tag{18}$$

with

$$C_{tH}^{(6)} = \frac{\lambda_t \lambda_T^2}{2}, \qquad C_{quH^5}^{(8)} = \frac{\lambda_t \lambda_T^2}{8}(4\lambda_t^2 - 3\lambda_T^2). \tag{19}$$

It is interesting to study the behaviors of $C_{tH}^{(6)}$ and $C_{quH^5}^{(8)}$ using the relationships of Eq. (9) and expanding in powers of $1/m_T$, keeping the top quark mass fixed to its physical value.[3] Note that keeping the top quark mass fixed rearranges the counting, as does alternatively using s_L and M_T as inputs. To $\mathcal{O}(1/m_T^4)$,

$$\begin{aligned}\lambda_t &= \frac{\sqrt{2}m_t}{v}\left\{1 + \frac{\lambda_T^2 v^2}{4m_T^2} + \frac{\lambda_T^2 v^2 m_t^2}{4m_T^4} - \frac{\lambda_T^4 v^4}{32 m_T^4}\right\} \\ &\to \frac{\sqrt{2}m_t}{c_L v}\left\{1 - s_L^2 \frac{m_t^2}{m_T^2} - s_L^4 \frac{m_t^4}{4m_T^4}\right\} \\ \bar{C}_6 &\equiv \frac{C_{tH}}{m_T^2} \\ &\to \frac{2m_t s_L^2}{\sqrt{2}c_L^3 v^3}\left(1 - \frac{(s_L^2+4)m_t^2}{2m_T^2} - \frac{(s_L^4 - 8s_L^2 - 8)m_t^4}{8m_T^4}\right) \\ \bar{C}_8 &\equiv \frac{C_{quH^5}}{m_T^4} \\ &\to \frac{m_t}{\sqrt{2}}\frac{s_L^2}{c_L^5 v^5}\left\{-3s_L^2 + \frac{m_t^2}{2m_T^2}(3s_L^4 + 24 s_L^2 + 8)\right. \\ &\quad \left. + \frac{m_t^4}{8m_T^4}(3s_L^6 - 48 s_L^4 - 192 s_L^2 - 64)\right\}. \end{aligned} \tag{20}$$

The naive scalings, $\bar{C}_6 \sim 1/m_T^2$ and $\bar{C}_8 \sim 1/m_T^4$, are modified by terms of $\mathcal{O}(s_L^2 x)$ when using the physical parameters.

Expanding Eq. (18) to linear order in the Higgs field, we define the top Yukawa, $Y_t^{(8)}$, as usual, as

[3]Note that we are free to take a combination of three Lagrangian and/or physical parameters as inputs.

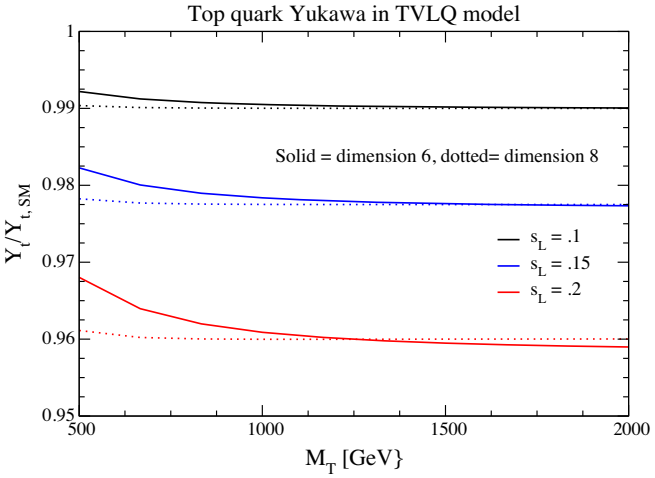

FIG. 3. Top quark Yukawa coupling normalized to the SM top quark Yukawa when dimension-eight contributions are included ($Y_t^{(8)}$) and when only dimension-six terms are included ($Y_t^{(6)}$).

$$\mathcal{L} \sim -\frac{Y_t^{(8)}}{\sqrt{2}} \bar{t}_L t_R h + \text{H.c.}, \tag{21}$$

where the superscript 8 denotes the inclusion of the dimension-eight contributions. We initially fix m_t (the physical top quark mass), λ_T, and $m_{\mathcal{T}}$,

$$\begin{aligned} Y_t^{(8)} &= \lambda_t - \frac{3v^2}{2}\bar{C}_6 - \frac{5v^4}{4}\bar{C}_8 \\ &= \frac{m_t\sqrt{2}}{v}\left\{1 - \frac{\lambda_T^2 v^2}{2m_{\mathcal{T}}^2} - \frac{m_t^2 v^2 \lambda_T^2}{m_{\mathcal{T}}^4} + \frac{\lambda_T^4 v^4}{4m_{\mathcal{T}}^4}\right\}, \end{aligned} \tag{22}$$

retaining only the dimension-six terms in the Lagrangian,

$$\begin{aligned} Y_t^{(6)} &= \lambda_t - \frac{3v^2}{2}\bar{C}_6 \\ &= \frac{m_t\sqrt{2}}{v}\left\{1 - \frac{\lambda_T^2 v^2}{2m_{\mathcal{T}}^2}\right\} + \mathcal{O}\left(\frac{1}{m_{\mathcal{T}}^4}\right). \end{aligned} \tag{23}$$

In Eqs. (22) and (23), the SM is recovered in the $\lambda_T^2/m_{\mathcal{T}}^2 \to 0$ limit, which corresponds to the $s_L \to 0$ limit. The choice to use m_t as an input introduces terms of $\mathcal{O}(\lambda_T^4/m_{\mathcal{T}}^4)$ in $Y_t^{(6)}$ due to the interdependence of the parameters.

In the small s_L limit,

$$\begin{aligned} Y_t^{(8)} &\to \frac{m_t\sqrt{2}}{v}\left\{1 - s_L^2 + \frac{3s_L^2 m_t^4}{m_{\mathcal{T}}^4}\right\} \\ Y_t^{(6)} &\to \frac{m_t\sqrt{2}}{v}\left\{1 - s_L^2 + \frac{5s_L^2 m_t^2}{2m_{\mathcal{T}}^2} - \frac{3s_L^2 m_t^4}{2m_{\mathcal{T}}^4}\right\}. \end{aligned} \tag{24}$$

We see that the SM limit is only recovered in the $s_L \to 0$ limit, consistent with the decoupling discussion in the previous section. Figure 3 shows the effect of including the dimension-eight terms on the top quark Yukawa coupling and we see that it is typically less than a few percent for 500 GeV $< m_{\mathcal{T}} <$ 1 TeV.

IV. PHENOMENOLOGY

We are now in a position to investigate the numerical effects of including the dimension-eight terms in the SMEFT analysis of the TVLQ and in the comparison between SMEFT and the UV complete model. As an example of the possible impact of the dimension-eight contributions, we consider $t\bar{t}h$ production at the 13 TeV LHC.[4] In addition to the SM cross section, $d\sigma_{\text{SM}}$, we consider various SMEFT expansions:

$$\begin{aligned} d\sigma_{\text{int}} &\sim \int (\text{dPS})\left\{|\mathcal{A}_{\text{SM}}|^2 + \frac{2}{\Lambda^2}\text{Re}\left(\sum C_i^{(6)}\mathcal{A}_i^{(6)}\mathcal{A}_{\text{SM}}^*\right)\right\} \\ d\sigma_6 &\sim \int (\text{dPS})\left\{|\mathcal{A}_{\text{SM}}|^2 + \frac{2}{\Lambda^2}\text{Re}\left(\sum C_i^{(6)}\mathcal{A}_i^{(6)}\mathcal{A}_{\text{SM}}^*\right)\right. \\ &\quad \left. + \frac{1}{\Lambda^4}\text{Re}\left(\sum_{i,j} C_i^{(6)}C_j^{(6)*}\mathcal{A}_i^{(6)}\mathcal{A}_j^{(6)*}\right)\right\} \\ d\sigma_8 &\sim \int (\text{dPS})\left\{|\mathcal{A}_{\text{SM}}|^2 + \frac{2}{\Lambda^2}\text{Re}\left(\sum C_i^{(6)}\mathcal{A}_i^{(6)}\mathcal{A}_{\text{SM}}^*\right)\right. \\ &\quad + \frac{1}{\Lambda^4}\text{Re}\left(\sum_{i,j} C_i^{(6)}C_j^{(6)*}\mathcal{A}_i^{(6)}\mathcal{A}_j^{(6)*}\right) \\ &\quad \left. + \frac{2}{\Lambda^4}\text{Re}\left(\sum_i C_i^{(8)}\mathcal{A}_i^{(8)}\mathcal{A}_{\text{SM}}^*\right)\right\}. \end{aligned} \tag{25}$$

In particular, $d\sigma_6$ and $d\sigma_8$ are of the same order in $1/\Lambda^4$ and the difference between the two is a measure of the importance of the dimension-eight terms. In our numerical studies, we will always take $\Lambda = m_{\mathcal{T}}$.

The rescaling of the top Yukawa coupling at dimension eight will give only a small difference from the dimension-six result as demonstrated in Fig. 3. However, the dimension-eight terms introduce a momentum dependence into the $t\bar{t}h$ and $t\bar{t}hg$ vertices, as well as the tbW and $tbWh$ vertices. The Feynman rules relevant for the $t\bar{t}h$ process are given in Appendix A. Note that, since there is never more than one covariant derivative operating on the top quark at dimension eight, the TVLQ model only generates new operators with a single gluon field. We use FeynRules [59,66] to generate the Feynman rules including the dimension-eight terms and use the resulting universal FeynRules output (UFO) [58] file with MADGRAPH5 and the default dynamical scale choice to generate events. For all our simulations, we

[4]The TVLQ model contributes to gluon fusion at one-loop, but a consistent inclusion of the dimension-eight contributions would require the double insertion of the dimension-six contributions. The contribution to $gg \to h$ from the TVLQ is suppressed by s_L^2 and is numerically small [65].

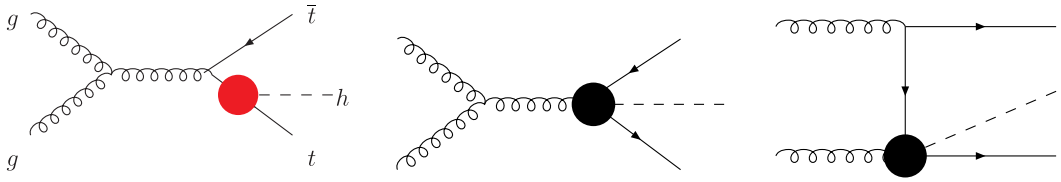

FIG. 4. Sample Feynman diagrams contributing to $gg \to t\bar{t}h$, including dimension-eight operators. The blobs represent the effects of the dimension-eight operators for the center and right-most diagrams, while the left-most diagram (red blob) receives contributions from both dimension-six and dimension-eight operators. Similar diagrams with $q\bar{q}$ initial states are not shown, but included in our computations.

set $m_t = 172$ GeV, $m_h = 125$ GeV, $m_Z = 91.1876$ GeV, $G_F = 1.16637 \times 10^{-5}$, and $\alpha = 1/127.9$, so that m_W is computed to be 79.82436 GeV at tree level in the MADGRAPH5 code. We use the NNPDF23 LO PDF set with $\alpha_s = 0.119$. The complete set of interactions can be found using the FeynRules module contained in the Supplemental Material [61].

We begin by considering the $t\bar{t}h$ process without decays. Some sample diagrams are shown in Fig. 4. There are two effects from the higher dimension operators. The first is the rescaling of the $t\bar{t}h$ Yukawa interaction. This does not lead to any momentum-dependent effects in the $gg \to t\bar{t}h$ process, but due to the small contributions from the $q\bar{q} \to t\bar{t}h$ subprocess, where the h couples to an intermediate Z boson (which are not rescaled by the top Yukawa), there are very small kinematic effects in the total cross section at the $\lesssim 1\%$ level. The second effect, which first arises at dimension eight, is interactions that are enhanced by an energy factor, $\sim s$ (with s being the partonic center of mass energy), relative to the SM contributions, both in the $t\bar{t}h$ and $t\bar{t}hg$ effective vertices. However, these s-enhanced contributions are proportional to a difference in the projection operators, $(P_R - P_L)$ [cf. Eq. (A2)], and the enhancement is therefore averaged out in the helicity blind production of on shell tops from QCD production. The resulting distributions for $t\bar{t}h$ production without decays are therefore essentially flat in various kinematic observables, and roughly consistent with an overall rescaling of the cross section by the modified top Yukawas in Eqs. (22) and (23).

We next consider $t\bar{t}h$ production with the tops decayed to the final state $b\bar{b}W^+W^-h$. We generate events in this final state from all tree-level diagrams including intermediate top quarks to exclude pure electroweak production of W and b pairs. This includes contributions from a number of diagrams which cannot be factorized into $t\bar{t}h$ production times decay. One example of such a diagram is shown in the right-hand side of Fig. 5. There are also contributions that are not proportional to the top Yukawa coupling, where the Higgs boson instead couples to the W bosons or bottom quarks.

We compute the cross section for $pp \to b\bar{b}W^+W^-h$ with intermediate top quarks using our FeynRules implementation, and plot the result in bins of $p_{T,h}$ in Fig. 6. We show results both for the SM, and with the SMEFT matched with $\lambda_T = 3.0$ and $m_{\mathcal{T}} = 2$ TeV, corresponding to a mixing angle $\sin\theta_L \sim 0.25$. We note that such large values of the mixing

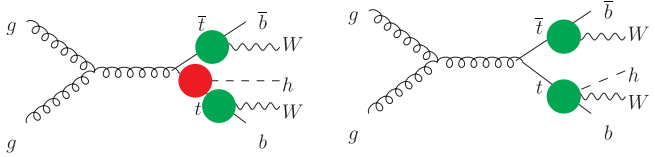

FIG. 5. Sample diagrams contributing to $gg \to b\bar{b}W^+W^-h$. The green blob represents the insertion of dimension-six operators, while the red blob represents both dimension-six and dimension-eight operators. Similar diagrams with $q\bar{q}$ initial states are not shown, but are included in our computations.

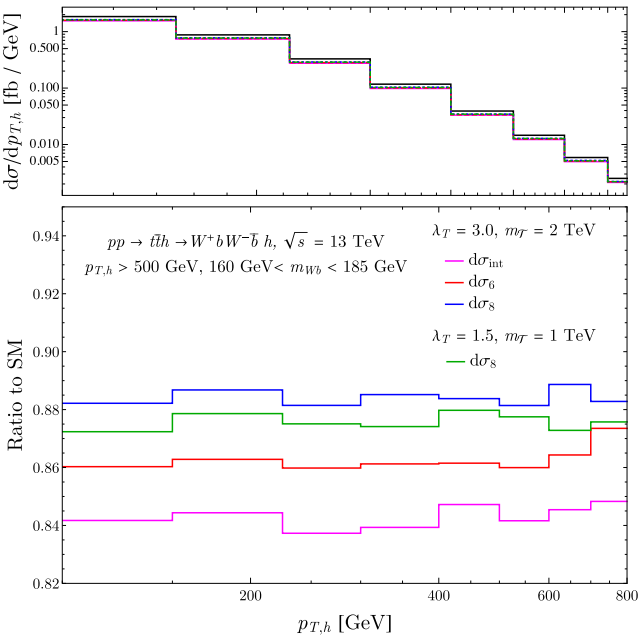

FIG. 6. The distribution for $W^+W^-b\bar{b}h$ production with intermediate top quarks in bins of the Higgs $p_{T,h}$. The top panel shows the distribution for the SM (black) and for the TVLQ point with $\lambda_T = 3.0$, $m_{\mathcal{T}} = 2$ TeV, matched to various orders in the SMEFT, as in Eq. (25), with the magenta, red, and blue curves representing $d\sigma_{\rm int}$, $d\sigma_6$, and $d\sigma_8$, respectively. The results for $d\sigma_8$ with $\lambda_T = 1.5$ and $m_{\mathcal{T}} = 1$ TeV are shown in green.

angle are excluded by fits to the oblique parameters (see Fig. 2)—we choose such a large point to make the kinematic effects that arise at different orders in the SMEFT expansion clear. To focus on the effects on $t\bar{t}h$ production, we impose a cut on the W boson and b quark system, requiring it to be near the top quark mass shell: 160 GeV $< m_{Wb} <$ 185 GeV. We utilize the charge information of the W and b particles in performing this cut, assuming that they can be properly assigned to the correct top quark in a true experimental analysis, e.g., if they are all identified in a single large-radius top jet.

Including the full $b\bar{b}W^+W^-h$ final state changes the expectations from $t\bar{t}h$ production without decays significantly. The diagrams where the Higgs is coupled to a W boson or b quark are not proportional to the top Yukawa, and therefore are not rescaled by the corrections to the top Yukawa as the bulk of the cross section is in the undecayed case. This leads to a growth in the cross section for large $p_{T,h}$ even at the dimension-six level, and a change in the overall rate that is significantly different from a naive rescaling. At dimension eight, there are nonfactorizable contributions with $thWb$ vertices, which have one fewer propagator than the SM-like diagrams, and, as a result, s-enhanced effects relative to the Standard Model. Finally, since the tops decay via their $SU(2)_L$ interactions, the effective operators proportional to $(P_R - P_L)$ discussed above will no longer be averaged out, and can therefore lead to additional effects at high $p_{T,h}$ as well. All of these effects in the amplitudes compete, and interfere, with one another.

The resulting effects in Fig. 6 show that the kinematic effects apparent at dimension six are nearly washed out at dimension eight, and the distribution is almost flat. We emphasize that, while the overall distribution is roughly flat in $p_{T,h}$, due to a combination of different effects that arise at different orders in the EFT expansion, the overall rate is different than that expected by rescaling the SM cross section by the modified top Yukawa. Note also that the size of the contributions from the dimension-eight operators are similar to the size of the dimension-six squared terms relative to the interference contribution alone.

We also include in Fig. 6 a curve in green, showing the results for matching up to dimension eight with $\lambda_T = 1.5$ and $m_T = 1$ TeV. These values are chosen such that the effects at dimension six in the SMEFT, which all scale as λ_T^2/m_T^2, are precisely the same as for $\lambda_T = 3.0$, $m_T = 2$ TeV. At dimension eight, however, there are effects that break this scaling [cf. Eqs. (22) and (A2)–(A4)], and we see that indeed, the dimension-eight curve in green is different than the curve in blue.

In Fig. 7, we show the distributions for $t\bar{t}h$ production including the full $b\bar{b}W^+W^-h$ final state in bins of $|\Delta\phi_{t\bar{t}}|$ and $|\Delta\eta_{t\bar{t}}|$, after placing a cut on the Higgs $p_{T,h} > 500$ GeV. We see there are no kinematic effects in these distributions at any order in the SMEFT expansion, other than the rescaling consistent with the results in Fig. 6.

Finally, we comment on the size of the dimension-eight effects for parameters that are not experimentally excluded. We take $\lambda_T = 1.5$ and $m_T = 2$ TeV, corresponding to a mixing angle $\sin\theta_L = 0.13$, which is near the edge of the region allowed by the oblique parameter fits shown in Fig. 2. For these parameters, the effects of the dimension-eight terms included in $d\sigma_8$ are very small: $\lesssim\mathcal{O}(1\%)$ of the SM cross section. The effects of the $\mathcal{O}(1/\Lambda^4)$ terms in $d\sigma_6$ are of similar size. There are small kinematic effects, but the total rate is quite similar to what one expects from a naive rescaling of the cross section by $(Y_t^{(6)})^2$. We conclude that the effects of the $\mathcal{O}(1/\Lambda^4)$ terms are too small to affect constraints on the TVLQ model at the LHC from tth production.

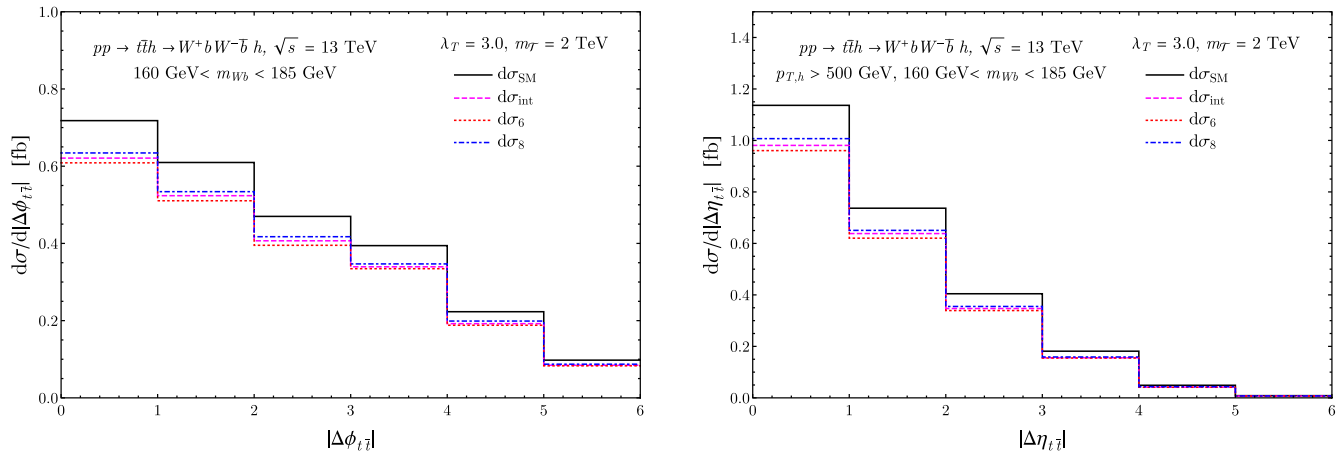

FIG. 7. The distribution for $W^+W^-b\bar{b}h$ production with intermediate top quarks in bins of $|\Delta\phi_{t\bar{t}}|$ (left) and $|\Delta\eta_{t\bar{t}}|$ (right), for events with $p_{T,h} > 500$ GeV, matched at various orders in the SMEFT expansion for $\lambda_T = 3.0$, $m_T = 2$ TeV. The black solid, magenta dashed, red dotted, and blue dot-dashed curves show the results for $d\sigma_{SM}$, $d\sigma_{int}$, $d\sigma_6$, and $d\sigma_8$, respectively.

V. DISCUSSION

We have implemented the complete dimension-eight set of operators contributing to the tree-level process, $pp \to t\bar{t}h$, in a model with a charge-2/3 vectorlike quark. When the decays of the top quark are not included, the results are almost entirely given by the rescaling of the top quark Yukawa coupling. The decays of the top quark introduce a momentum dependence due primarily to the presence of nonfactorizable $tbWh$ vertices. These effects create a difference of less than $\mathcal{O}(2\%)$ at high $p_{T,h}$ between the square of the dimension-six contributions and the result with the dimension-eight contributions included.

The example we have considered is particularly simple, since the input parameters are not rescaled at tree level to dimension eight. It would be of interest to consider the effects of a more complicated model which generates tree-level rescaling of the input parameters at dimension eight. The results of Refs. [20,67] suggest that the dimension-eight contributions may play a more significant role in such scenarios.

The UFO and FeynRules model files used to generate the TVLQ dimension-eight effects are included as Supplemental Material [61].

ACKNOWLEDGMENTS

S. D. and M. S. are supported by the United States Department of Energy under Grant Contract No. DE-SC0012704. S. H. is supported in part by the DOE Grant No. DE-SC0013607, and in part by the Alfred P. Sloan Foundation Grant No. G-2019-12504. Digital data is contained in the Supplemental Material [61] submitted with this paper.

APPENDIX A: DIMENSION-EIGHT INTERACTIONS

The following terms in the tree-level dimension-eight Lagrangian, $\mathcal{L}_8'$, contain non-SM gluon couplings:

$$\begin{aligned}\mathcal{L}_{8,g} = {} & i\frac{\lambda_T^2}{m_T^4}(\bar{\psi}_L D^\mu \tilde{H})\gamma_\mu(D^\nu \tilde{H}^\dagger D_\nu \psi_L) + i\frac{\lambda_T^2}{m_T^4}(\bar{\psi}_L \tilde{H})\gamma_\mu(D^\mu D^\nu \tilde{H}^\dagger D_\nu \psi_L) \\ & - i\frac{\lambda_T^2}{m_T^4}(\bar{\psi}_L \tilde{H})\gamma_\mu(D^\nu D^\mu \tilde{H}^\dagger D_\nu \psi_L) - \frac{\lambda_t \lambda_T^2}{m_T^4}(H^\dagger H)\bar{t}_R(D^\mu \tilde{H}^\dagger D_\mu \psi_L) + \text{H.c.},\end{aligned} \tag{A1}$$

where indices are contracted implicitly such that terms in parentheses are $SU(2)$ singlets. The $t\bar{t}h$ interactions that are needed for the tree-level process are (with all momenta outgoing),

$$\begin{aligned} t(p_1)\bar{t}(p_2)h(p_h) &= -i\frac{Y_t^{(8)}}{\sqrt{2}} + i\frac{\lambda_T^2 v m_t}{4m_T^4}(p_1 - p_2)\cdot p_h(P_R - P_L) \\ t(p_1)\bar{t}(p_2)h(p_h)g^{A\mu}(p_g) &= ig_s\frac{\lambda_T^2 v m_t}{2m_T^4}p_h^\mu T^A(P_R - P_L), \end{aligned} \tag{A2}$$

where $P_{L,R} \equiv \frac{1}{2}(1 \mp \gamma_5)$ and $Y_t^{(8)}$ is as given in Eq. (22).

The following are the electroweak couplings of the top quark expanded to dimension eight that occur in the $t\bar{t}h, t \to Wb$ process:

$$\begin{aligned} b(p_b)\bar{t}(p_t)W^{+\mu}(p_W) = {} & i\frac{g_W}{\sqrt{2}}\gamma^\mu P_L\left[1 - \frac{v^2\lambda_T^2}{4{m_T}^2} + \frac{v^2\lambda_T^2}{32{m_T}^4}(3v^2\lambda_T^2 + 8(m_t^2 - p_t^2 + p_b^2))\right] \\ & - i\frac{g_W v^2 \lambda_T^2}{2\sqrt{2}{m_T}^4}p_b^\mu P_R[m_t - \not{p}_W], \end{aligned} \tag{A3}$$

$$\begin{aligned} b(p_b)\bar{t}(p_t)W^{+\mu}(p_W)h(p_h) = {} & -\frac{ivg_W\lambda_T^2\gamma^\mu P_L}{2\sqrt{2}{m_T}^2}\left[1 + \frac{p_h\cdot p_t}{{m_T}^2} + \frac{2p_b\cdot p_W}{{m_T}^2} + \frac{p_h^2}{2{m_T}^2} + \frac{p_W^2}{{m_T}^2} + \frac{p_h\cdot p_W}{{m_T}^2}\right. \\ & \left. - \frac{3v^2\lambda_T^2}{4{m_T}^2} - \frac{2m_t^2}{{m_T}^2} - \frac{\not{p}_h\not{p}_W}{2{m_T}^2} - \frac{m_t\not{p}_h}{2m_T^2}\right] \\ & + \frac{ivg_W\lambda_T^2 P_R}{2\sqrt{2}{m_T}^4}[p_b^\mu(\not{p}_h + 2\not{p}_W - 3m_t) - p_h^\mu(\not{p}_h + \not{p}_W - m_t)]. \end{aligned} \tag{A4}$$

APPENDIX B: T PARAMETER IN EFFECTIVE FIELD THEORY LANGUAGE

The oblique parameter $\Delta\mathcal{T}$ has been calculated some time ago for the TVLQ model [65]. It is instructive to revisit this calculation using an effective field theory framework [68] and it is an example of the importance of including the one-loop matching in SMEFT calculations. The contributions to $\Delta\mathcal{T}$ from fermions with masses m_1 and m_2 can be expressed in terms of the function

$$\begin{aligned}\theta_+(y_1,y_2) = y_1+y_2 &- \frac{2y_1y_2}{y_1-y_2}\log\left(\frac{y_1}{y_2}\right)\\ &- 2(y_1\log(y_1)+y+2\log(y_2))\\ &- 2(y_1+y_2)\frac{1}{\epsilon}\left(\frac{4\pi\mu^2}{M_Z^2}\right)^{\epsilon},\end{aligned} \tag{B1}$$

where $y_i = m_i^2/M_Z^2$ and μ is an arbitrary renormalization scale. Neglecting the b quark mass and taking $m_t \gg M_Z$, the $t-b$ contribution to the SM is found from the diagrams of Fig. 8 with SM fermion-gauge boson couplings,

$$\mathcal{T}_{\rm SM} = \frac{3}{16\pi s_W^2 c_W^2} y_t \tag{B2}$$

with $c_W \equiv M_W/M_Z$.

At the UV scale (which here we take to be the physical mass of the TVLQ, M_T), we integrate out the contributions of the diagrams of Fig. 9 using the couplings from Ref. [37] to obtain the contribution from heavy fermions, $\mathcal{T}_H$,

$$\begin{aligned}\mathcal{T}_H(\mu) &= T_{\rm SM}s_L^2(\theta_+(y_T,y_b) - c_L^2\theta_+(y_T,y_t) - \frac{1}{2}\theta_+(y_T,y_T))\\ &= T_{\rm SM}s_L^2\left\{s_L^2\frac{M_T^2}{m_t^2} - c_L^2 + \frac{2c_L^2}{\epsilon} + 2c_L^2\log\left(\frac{M_T^2}{\mu^2}\right)\right\}.\end{aligned} \tag{B3}$$

For the UV matching, the appropriate scale is $\mu = M_T$, giving the contribution

$$\mathcal{T}_H(M_T) = T_{\rm SM}s_L^2\left\{s_L^2\frac{M_T^2}{m_t^2} - c_L^2 + \frac{2c_L^2}{\epsilon}\right\}. \tag{B4}$$

Equation (B4) exhibits the familiar decoupling requirement that $s_L^2 M_T^2/m_t^2 \ll 1$.

We identify

$$\mathcal{T}(\mu) = -\frac{v^2}{2\alpha}\frac{C_{HD}^{(6)}(\mu)}{\Lambda^2}, \tag{B5}$$

where $O_{HD} = |H^\dagger D_\mu H|^2$. The coefficient function must be renormalization group evolved to the low energy scale which we take to be m_t. In the TVLQ, only the top quark Yukawa coupling contributes, and we have [69]

$$C_{HD}(m_t) = C_{HD}(M_T) + \frac{\dot{C}_{HD}}{16\pi^2}\log\left(\frac{m_t}{M_T}\right), \tag{B6}$$

with the TVLQ result

$$\dot{C}_{HD} = 24 C_{Ht}^{(1)}\hat{Y}_t^2, \tag{B7}$$

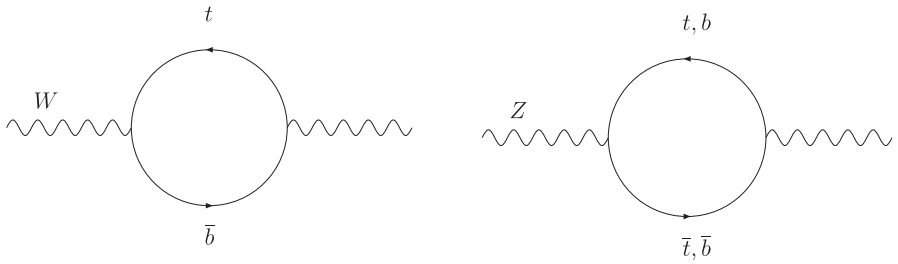

FIG. 8. Feynman diagrams contributing to the $\mathcal{T}$ parameter from SM fermions.

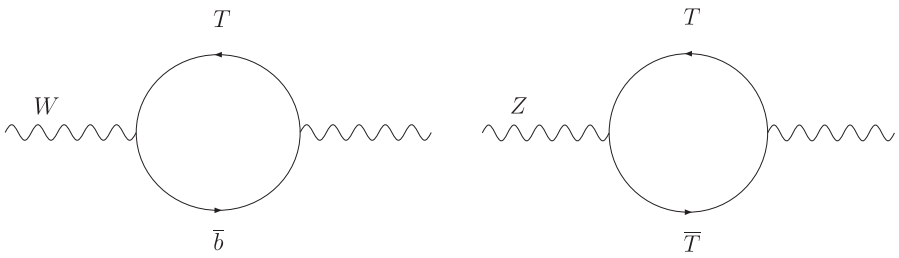

FIG. 9. Feynman diagrams contributing to the $\mathcal{T}$ parameter from the heavy $TVLQ$ fermion, T.

where $\hat{Y}_t = \sqrt{2}c_L m_t/v$ is the top Yukawa at the UV matching scale. Equation (B4) yields

$$\mathcal{T}_H(m_t) = T_{\rm SM} s_L^2 \left\{ s_L^2 \frac{M_T^2}{m_t^2} - c_L^2 + \frac{2c_L^2}{\epsilon} - 2c_L^2 \log\left(\frac{m_t^2}{M_T^2}\right) \right\}. \tag{B8}$$

Finally, at the low scale m_t, we need to include the diagrams of Fig. 9 and subtract off the SM $t-b$ contribution,

$$\mathcal{T}_L(m_t) - \mathcal{T}_{\rm SM} = \mathcal{T}_{\rm SM} s_L^2 \left(-1 - \frac{2c_L^2}{\epsilon}\right). \tag{B9}$$

Adding together Eqs. (B8) and (B9), we see that the effective field theory approach with one-loop matching reproduces the correct result,

$$\begin{aligned}\Delta\mathcal{T} &= \mathcal{T}(m_t)_H + \mathcal{T}_L(m_t) - \mathcal{T}_{\rm SM} \\ &= T_{\rm SM} s_L^2 \left\{ s_L^2 \frac{M_T^2}{m_t^2} - c_L^2 - 1 + 2c_L^2 \log\left(\frac{M_T^2}{m_t^2}\right) \right\}. \end{aligned} \tag{B10}$$

To put Eq. (B10) into the language of the dimension-six SMEFT, we note that

$$\begin{aligned} s_L^2 &= \frac{2v^2 C_{Ht}^{1,(6)} v^2}{M_T^2} + \mathcal{O}\left(\frac{v^4}{m_T^4}\right) \\ c_L^2 &= 1 + \mathcal{O}\left(\frac{v^4}{m_T^4}\right) \\ s_L^4 \frac{M_T^2}{m_t^2} &= \frac{4[C_{Ht}^{1,(6)}]^2 v^4}{M_T^2 m_t^2} + \mathcal{O}\left(\frac{v^4}{m_T^4}, \frac{v^4}{m_T^2 m_t^2}\right). \end{aligned} \tag{B11}$$

Since we compute only single insertions of operators, Eq. (B10) becomes

$$\begin{aligned}\Delta\mathcal{T}_{\rm SMEFT} = 2T_{\rm SM} \frac{v^2 C_{Ht}^{1,(6)}}{M_T^2} \left\{ -2 + 2\log\left(\frac{M_T^2}{m_t^2}\right) \right\} \\ + \mathcal{O}\left(\frac{v^4}{m_T^4}, \frac{v^4}{m_T^2 m_t^2}\right). \end{aligned} \tag{B12}$$

[1] I. Brivio and M. Trott, The standard model as an effective field theory, Phys. Rep. **793**, 1 (2019).
[2] S. Dawson and P. P. Giardino, Electroweak and QCD corrections to Z and W pole observables in the Standard Model EFT, Phys. Rev. D **101**, 013001 (2020).
[3] J. J. Ethier, G. Magni, F. Maltoni, L. Mantani, E. R. Nocera, J. Rojo, E. Slade, E. Vryonidou, and C. Zhang, Combined SMEFT interpretation of Higgs, diboson, and top quark data from the LHC, arXiv:2105.00006.
[4] E. d. S. Almeida, A. Alves, O. J. P. Éboli, and M. C. Gonzalez-Garcia, Electroweak legacy of the LHC Run II, arXiv:2108.04828.
[5] R. Contino, A. Falkowski, F. Goertz, C. Grojean, and F. Riva, On the validity of the effective field theory approach to SM precision tests, J. High Energy Phys. 07 (2016) 144.
[6] L. Berthier and M. Trott, Consistent constraints on the standard model effective field theory, J. High Energy Phys. 02 (2016) 069.
[7] G. Panico, F. Riva, and A. Wulzer, Diboson interference resurrection, Phys. Lett. B **776**, 473 (2018).
[8] W. Buchmuller and D. Wyler, Effective lagrangian analysis of new interactions and flavor conservation, Nucl. Phys. **B268**, 621 (1986).
[9] J. Ellis, S.-F. Ge, H.-J. He, and R.-Q. Xiao, Probing the scale of new physics in the $zz\gamma$ coupling at e^+e^- colliders, Chin. Phys. C **44**, 063106 (2020).
[10] C. Hays, A. Martin, V. Sanz, and J. Setford, On the impact of dimension-eight SMEFT operators on Higgs measurements, J. High Energy Phys. 02 (2019) 123.
[11] C. W. Murphy, Dimension-8 operators in the standard model effective field theory, J. High Energy Phys. 10 (2020) 174.
[12] C. W. Murphy, Low-energy effective field theory below the electroweak scale: Dimension-8 operators, J. High Energy Phys. 04 (2021) 101.
[13] H.-L. Li, Z. Ren, M.-L. Xiao, J.-H. Yu, and Y.-H. Zheng, Low energy effective field theory operator basis at d $\leq$ 9, J. High Energy Phys. 06 (2021) 138.
[14] H.-L. Li, Z. Ren, J. Shu, M.-L. Xiao, J.-H. Yu, and Y.-H. Zheng, Complete set of dimension-eight operators in the Standard Model effective field theory, Phys. Rev. D **104**, 015026 (2021).
[15] S. Dawson, I. M. Lewis, and M. Zeng, Usefulness of effective field theory for boosted Higgs production, Phys. Rev. D **91**, 074012 (2015).
[16] S. Dawson, I. M. Lewis, and M. Zeng, Effective field theory for Higgs boson plus jet production, Phys. Rev. D **90**, 093007 (2014).
[17] R. V. Harlander and T. Neumann, Probing the nature of the Higgs-gluon coupling, Phys. Rev. D **88**, 074015 (2013).
[18] M. Grazzini, A. Ilnicka, M. Spira, and M. Wiesemann, Modeling BSM effects on the Higgs transverse-momentum spectrum in an EFT approach, J. High Energy Phys. 03 (2017) 115.

[19] M. Battaglia, M. Grazzini, M. Spira, and M. Wiesemann, Sensitivity to BSM effects in the Higgs p_T spectrum within SMEFT, arXiv:2109.02987.
[20] T. Corbett, A. Helset, A. Martin, and M. Trott, EWPD in the SMEFT to dimension eight, J. High Energy Phys. 06 (2021) 076.
[21] S. Dawson, S. Homiller, and S. D. Lane, Putting standard model EFT fits to work, Phys. Rev. D **102**, 055012 (2020).
[22] I. Brivio, S. Bruggisser, E. Geoffray, W. Kilian, M. Krämer, M. Luchmann, T. Plehn, and B. Summ, From models to SMEFT and back? arXiv:2108.01094.
[23] N. Arkani-Hamed, A. G. Cohen, E. Katz, and A. E. Nelson, The littlest Higgs, J. High Energy Phys. 07 (2002) 034.
[24] M. Perelstein, M. E. Peskin, and A. Pierce, Top quarks and electroweak symmetry breaking in little Higgs models, Phys. Rev. D **69**, 075002 (2004).
[25] C. Csaki, J. Hubisz, G. D. Kribs, P. Meade, and J. Terning, Big corrections from a little Higgs, Phys. Rev. D **67**, 115002 (2003).
[26] G. Panico and A. Wulzer, The Composite Nambu-Goldstone Higgs, Lect. Notes Phys. **913**, 1 (2016).
[27] O. Matsedonskyi, G. Panico, and A. Wulzer, Top partners searches and composite Higgs models, J. High Energy Phys. 04 (2016) 003.
[28] B. A. Dobrescu and C. T. Hill, Electroweak Symmetry Breaking via a Top Condensation Seesaw Mechanism, Phys. Rev. Lett. **81**, 2634 (1998).
[29] H.-J. He, C. T. Hill, and T. M. P. Tait, Top quark seesaw model, vacuum structure, and electroweak precision constraints, Phys. Rev. D **65**, 055006 (2002).
[30] M. K. Gaillard, The effective one loop lagrangian with derivative couplings, Nucl. Phys. **B268**, 669 (1986).
[31] B. Henning, X. Lu, and H. Murayama, How to use the standard model effective field theory, J. High Energy Phys. 01 (2016) 023.
[32] W. Beenakker, S. Dittmaier, M. Kramer, B. Plumper, M. Spira, and P. M. Zerwas, Higgs Radiation Off Top Quarks at the Tevatron and the LHC, Phys. Rev. Lett. **87**, 201805 (2001).
[33] W. Beenakker, S. Dittmaier, M. Kramer, B. Plumper, M. Spira, and P. M. Zerwas, NLO QCD corrections to t anti-t H production in hadron collisions, Nucl. Phys. **B653**, 151 (2003).
[34] S. Dawson, L. H. Orr, L. Reina, and D. Wackeroth, Associated top quark Higgs boson production at the LHC, Phys. Rev. D **67**, 071503 (2003).
[35] S. Dawson, C. Jackson, L. H. Orr, L. Reina, and D. Wackeroth, Associated Higgs production with top quarks at the large hadron collider: NLO QCD corrections, Phys. Rev. D **68**, 034022 (2003).
[36] G. Cacciapaglia, A. Deandrea, D. Harada, and Y. Okada, Bounds and decays of new heavy vector-like top partners, J. High Energy Phys. 11 (2010) 159.
[37] C.-Y. Chen, S. Dawson, and E. Furlan, Vectorlike fermions and Higgs effective field theory revisited, Phys. Rev. D **96**, 015006 (2017).
[38] G. Cacciapaglia, A. Carvalho, A. Deandrea, T. Flacke, B. Fuks, D. Majumder, L. Panizzi, and H.-S. Shao, Next-to-leading-order predictions for single vector-like quark production at the LHC, Phys. Lett. B **793**, 206 (2019).
[39] M. Buchkremer, G. Cacciapaglia, A. Deandrea, and L. Panizzi, Model independent framework for searches of top partners, Nucl. Phys. **B876**, 376 (2013).
[40] G. Cacciapaglia, A. Deandrea, L. Panizzi, N. Gaur, D. Harada, and Y. Okada, Heavy vector-like top partners at the LHC and flavour constraints, J. High Energy Phys. 03 (2012) 070.
[41] O. Matsedonskyi, G. Panico, and A. Wulzer, On the interpretation of top partners searches, J. High Energy Phys. 12 (2014) 097.
[42] F. del Aguila, J. A. Aguilar-Saavedra, and R. Miquel, Constraints on Top Couplings in Models with Exotic Quarks, Phys. Rev. Lett. **82**, 1628 (1999).
[43] J. A. Aguilar-Saavedra, Effects of mixing with quark singlets, Phys. Rev. D **67**, 035003 (2003); Erratum, Phys. Rev. D **69**, 099901 (2004).
[44] J. A. Aguilar-Saavedra, R. Benbrik, S. Heinemeyer, and M. Pérez-Victoria, Handbook of vectorlike quarks: Mixing and single production, Phys. Rev. D **88**, 094010 (2013).
[45] S. A. R. Ellis, R. M. Godbole, S. Gopalakrishna, and J. D. Wells, Survey of vector-like fermion extensions of the Standard Model and their phenomenological implications, J. High Energy Phys. 09 (2014) 130.
[46] F. d. Aguila, J. Santiago, and M. Perez-Victoria, Observable contributions of new exotic quarks to quark mixing, J. High Energy Phys. 09 (2000) 011.
[47] C.-Y. Chen, S. Dawson, and I. M. Lewis, Top partners and Higgs boson production, Phys. Rev. D **90**, 035016 (2014).
[48] M. Buchkremer, G. Cacciapaglia, A. Deandrea, and L. Panizzi, Model-independent framework for searches of top partners, Nucl. Phys. **B876**, 376 (2013).
[49] M. S. Chanowitz, M. A. Furman, and I. Hinchliffe, Weak interactions of ultra heavy fermions. 2., Nucl. Phys. **B153**, 402 (1979).
[50] M. Aaboud *et al.* (ATLAS Collaboration), Combination of the Searches for Pair-Produced Vector-Like Partners of the Third-Generation Quarks at $\sqrt{s} = 13$ TeV with the ATLAS Detector, Phys. Rev. Lett. **121**, 211801 (2018).
[51] A. M. Sirunyan, A. Tumasyan, W. Adam, F. Ambrogi, E. Asilar, T. Bergauer, J. Brandstetter, E. Brondolin, M. Dragicevic *et al.*, Search for vector-like t and b quark pairs in final states with leptons at $\sqrt{s} = 13$ tev, J. High Energy Phys. 08 (2018) 177.
[52] Y.-B. Liu and S. Moretti, Search for single production of a top quark partner via the $T \to th$ and $h \to WW*$ channels at the LHC, Phys. Rev. D **100**, 015025 (2019).
[53] B. Yang, M. Wang, H. Bi, and L. Shang, Single production of vectorlike T quark decaying into Wb at the LHC and the future pp colliders, Phys. Rev. D **103**, 036006 (2021).
[54] M. Aaboud *et al.* (ATLAS Collaboration), Search for single production of vector-like T quarks decaying to Ht or Zt in pp collisions $\sqrt{s} = 13$ TeV with the ATLAS detector, http://cdsweb.cern.ch/record/2779174/files/ATLAS-CONF-2021-040.pdf.
[55] A. J. Buras, C. Grojean, S. Pokorski, and R. Ziegler, FCNC effects in a minimal theory of fermion masses, J. High Energy Phys. 08 (2011) 028.
[56] J. C. Criado and M. Pérez-Victoria, Field redefinitions in effective theories at higher orders, J. High Energy Phys. 03 (2019) 038.

[57] I. Brivio and M. Trott, Scheming in the SMEFT... and a reparameterization invariance!, J. High Energy Phys. 07 (2017) 148; 05 (2018) 136(A).
[58] C. Degrande, C. Duhr, B. Fuks, D. Grellscheid, O. Mattelaer, and T. Reiter, Ufo- the universal feynrules output, Comput. Phys. Commun. **183**, 1201 (2012).
[59] A. Alloul, N. D. Christensen, C. Degrande, C. Duhr, and B. Fuks, Feynrules2.0, a complete toolbox for tree level phenomenology, Comput. Phys. Commun. **185**, 2250 (2014).
[60] B. Grzadkowski, M. Iskrzy?ski, M. Misiak, and J. Rosiek, Dimension-six terms in the standard model lagrangian, J. High Energy Phys. 10 (2010) 085.
[61] See Supplemental Material at http://link.aps.org/supplemental/10.1103/PhysRevD.104.115013 for the complete Feynrules output to dimension-eight.
[62] J. Brehmer, A. Freitas, D. Lopez-Val, and T. Plehn, Pushing Higgs effective theory to its limits, Phys. Rev. D **93**, 075014 (2016).
[63] D. Egana-Ugrinovic and S. Thomas, Effective theory of Higgs sector vacuum states, arXiv:1512.00144.
[64] H. Belusca-Maito, A. Falkowski, D. Fontes, J. C. Romao, and J. P. Silva, Higgs eft for 2hdm and beyond, Eur. Phys. J. C **77**, 176 (2017).
[65] S. Dawson and E. Furlan, A Higgs conundrum with vector fermions, Phys. Rev. D **86**, 015021 (2012).
[66] N. D. Christensen and C. Duhr, Feynrules: Feynman rules made easy, Comput. Phys. Commun. **180**, 1614 (2009).
[67] T. Corbett and T. Rasmussen, Higgs decays to two leptons and a photon beyond leading order in the SMEFT, arXiv:2110.03694.
[68] F. del Aguila, Z. Kunszt, and J. Santiago, One-loop effective lagrangians after matching, Eur. Phys. J. C **76**, 244 (2016).
[69] E. E. Jenkins, A. V. Manohar, and M. Trott, Renormalization group evolution of the standard model dimension six operators II: Yukawa dependence, J. High Energy Phys. 01 (2014) 035.